Journal of Power Sources 195 (2010) 3002–3010

Contents lists available at ScienceDirect

Journal of Power Sources

journal homepage: www.elsevier.com/locate/jpowsour

Triphenylamine- and benzothiadiazole-based dyes with multiple acceptors for application in dye-sensitized solar cells

John A. Mikroyannidis[a,*], P. Suresh[b], M.S. Roy[c], G.D. Sharma[b,d,**]

[a] Chemical Technology Laboratory, Department of Chemistry, University of Patras, GR-26500 Patras, Greece
[b] Physics Department, Molecular Electronic and Optoelectronic Device Laboratory, JNV University, Jodhpur, Rajasthan 342005, India
[c] Defence Laboratory, Jodhpur, Rajasthan 342011, India
[d] Jaipur Engineering College, Kukas, Jaipur, Rajasthan, India

ARTICLE INFO

Article history:
Received 11 August 2009
Received in revised form 21 October 2009
Accepted 26 October 2009
Available online 13 November 2009

Keywords:
Dye-sensitized solar cells (DSSCs)
Triphenylamine
Benzothiadiazole
Acceptor moiety
Nanocrystalline TiO_2 and ZTO
Polymer gel electrolyte

ABSTRACT

Two novel dyes TPAR3 and BTDR2 based on triphenylamine and benzothiadiazole, respectively, with multiple electron acceptors were synthesized and characterized by FT-IR, ^{1}H NMR, TGA and thermomechanical analysis (TMA). They carried terminal cyanoacrylic acid electron acceptors/anchoring moieties, which were connected with the central unit through a thiophene ring. The absorption bands of the dyes were extended up to ~570 nm with long-wave absorption maximum at 425–455 nm and optical band gap of 2.10–2.17 eV. The dyes emitted yellow–orange light with photoluminescence maximum at 547–615 nm. We have investigated the photovoltaic properties of quasi solid state dye sensitized solar cells (DSSCs) based on these metal free organic dyes. It has been found that the power conversion efficiency of the DSSCs based on composite zinc titanium oxide (ZTO) nanocrystalline photoelectrode is higher than that for TiO_2 based DSSCs. This has been attributed to the longer electron lifetime and more negative conduction band edge of ZTO. The overall power conversion efficiency of the DSSCs based on TPAR3 and BTDR2 employing ZTO photoelectrode is 6.3% and 3.6%, respectively. These results indicate that both the acceptor moiety of metal free organic dyes and ZTO photoelectrode have an effect on the photovoltaic performance of DSSCs.

1. Introduction

Dye-sensitized solar cells (DSSCs) have received attention for transferring clean solar energy into electricity over the past decade [1,2]. The inorganic–organic hybrid DSSCs have been extensively investigated for the areas of designing more efficient dyes and electron mediators [2], fabricating better nanostructured films [3], and more deeply understanding the interfacial charge-transfer process [3–5]. In a DSSC device, light is absorbed by the dye anchored on the TiO_2 surface and then electrons from the excited dye are injected into the conduction band of the TiO_2, generating electric current, while the ground state of the dye is regenerated by the electrolyte to give efficient charge-separation [6]. Thus, the dye in DSSCs is essential for efficient light harvesting and electron generation/transfer. The electrolyte, containing a redox couple I_3^-/I^- mediator, is injected into the slit between the anode and the catalytic Pt counter-electrode. A dye sensitizer needs efficient charge injection with photoexcitation [2]. To obtain high conversion efficiencies, it requires that the photogenerated electrons flow into the oxide film with minimal losses to interfacial recombination [3–5]. Up to now, DSSCs based on Ru-complex photosensitizers have exhibited the highest photo-to-current conversion efficiency and long-term chemical stability [6], while metal-free organic dyes have also been concerned due to their low cost [7,8].

Generally, metal-free organic dyes possess the evident molecular structure of the donor part and the acceptor part bridged by the conjugated chain. As far as donor parts are concerned, triphenylamine (TPA) and its derivatives have shown promising applications in the development of photovoltaic devices [9,10]. As the excited electrons on the dye molecules are injected to the semiconductor film through the acceptor moiety [11], the acceptor part has significant influence on the photovoltaic properties of the dyes. For example, Ito et al. employed rhodanine-3-acetic acid as the acceptor on indoline-based dye and attained the overall conversion efficiency of 9.03%, which was the highest value among the metal-free organic dyes so far [12]. Hara et al. used cyanoacrylic acid as the acceptor on coumarin-based dyes to investigate the influence of the different donor parts and got the overall efficiency range from

* Corresponding author. Tel.: +30 2610 997115; fax: +30 2610 997118.
** Corresponding author at: Physics Department, Molecular Electronic and Optoelectronic Device Laboratory, JNV University, Jodhpur, Rajasthan 342005, India. Tel.: +91 0291 2720857; fax: +91 0291 2720856.
E-mail addresses: mikroyan@chemistry.upatras.gr, mikroyan@googlemail.com (J.A. Mikroyannidis), sharmagd_in@yahoo.com (G.D. Sharma).

0378-7753/$ – see front matter © 2009 Elsevier B.V. All rights reserved.
doi:10.1016/j.jpowsour.2009.10.107

3.1% to 7.7% [13,14]. Recently, Chen and co-workers have reported a serial of TPA based organic dyes, showing that extending the π-conjugation of the donor part could improve the photovoltaic performance of the DSSCs [15–17]. Very recently, certain other groups [18–25] have reported DSSCs with various triphenylamine based dyes, indicating the importance of their further investigation in this topic.

Benzothiadiazole based polymers and small molecules have been widely employed in photovoltaic applications. However, a literature survey revealed that benzothiazole or benzoselenadiazole based polymers or small molecules have not been extensively used for DSSCs [26–29].

TiO_2 is a well-known and suitable material to fabricate the photoanode of DSSCs. To improve the efficiency of the DSSCs, other photoelectrodes have also been investigated. Wang et al., have reported high efficient DSSCs using a powder ZnO covered TiO_2 photoelectrode using a powder prepared from mixture of $ZnCl_2$ and $TiCl_4$ as photoanode for DSSC [30]. Saeki et al. [31] prepared titanium–zinc mixed oxide films by thermal oxidation and studied their photo-electrochemical properties. They observed that the photocurrent values were higher for these photoelectrodes than for the thermally formed TiO_2 photoelectrodes. Recently, Wu et al., reported that when $BaTiO_3$ modified TiO_2 photoelectrode is used for the DSSCs, the conversion efficiency significantly improves, which was attributed to the increase in V_{oc} due to the shift in conduction band edge of TiO_2 in negative direction after $BaTiO_3$ modification [32].

Although the DSSCs based on liquid electrolytes have reached high efficiency, the use of liquid electrolyte has created lot of difficulties in sealing and long term photo-chemical stability of the device because of easy volatile and decomposition of organic liquid electrolyte [33]. To overcome these problems, many efforts have been made in replacing the liquid electrolytes with solid or quasi solid-state electrolytes such as solid polymer electrolytes and polymer gel electrolytes [34–36].

In this investigation we describe the synthesis and characterization of triphenylamine- or benzothiadiazole-based dyes with multiple acceptors and their application as sensitizers in DSSCs. The triphenylamine-based dye (TPAR3) is a star shaped molecule with three terminal cyanoacrylic acid anchoring moieties. The benzothiadiazole-based dye (BTDR2) is a linear molecule with two terminal cyanoacrylic acid anchoring moieties. A thiophene ring, which acts as π-conjugated segment, connects each arm or side of the central unit with the terminal cyanoacrylic acid moieties. Triphenylamine is a better electron donor than the electron deficient benzothiadiazole. Triphenylamine also is expected to enhance the hole transporting properties of TPAR3. Moreover, the three-dimensional structure of triphenylamine will restrict the formation of dye aggregation on the semiconductor surface, which reduces the conversion efficiency of DSSCs [17]. The photophysical, electrochemical and photovoltaic properties of the two dyes were systematically investigated and correlated with their chemical structures. We report the preparation of DSSCs using BDTR2 and TPAR3 as sensitizer, on a photoelectrode with composite zinc titanium oxide (ZTO), poly(3,4-ethylenedioxythiophene) poly(styrenesulfonate) (PEDOT:PSS) conductive polymer as counter electrolyte and polymer gel electrolyte. The performance of this device has been compared with DSSCs consisted of only bare TiO_2 photoelectrode. Electrochemical impedance spectroscopy has been employed to get information about the factors, responsible for the performance of DSSCs. The results have shown that the presence of ZTO electrode in the DSSCs resulted the shifting of conduction band edge to more negative and longer electron lifetime, reduces the recombination between electrons and triiodide ions at the interface and improves the power conversion efficiency of the DSSCs.

2. Experimental

2.1. Characterization methods

IR spectra were recorded on a PerkinElmer 16PC FT-IR spectrometer with KBr pellets. ^{1}H NMR (400 MHz) spectra were obtained using a Brucker spectrometer. Chemical shifts (δ values) are given in parts per million with tetramethylsilane as an internal standard. UV–vis spectra were recorded on a Beckman DU-640 spectrometer with spectrograde THF. TGA was performed on a DuPont 990 thermal analyzer system. Ground samples of about 10 mg each were examined by TGA and the weight loss comparisons were made between comparable specimens. Dynamic TGA measurements were made at a heating rate of 20 °C min^{-1} in atmospheres of N_2 at a flow rate of 60 cm^3 min^{-1}. Thermomechanical analysis (TMA) was recorded on a DuPont 943 TMA using a loaded penetration probe at a scan rate of 20 °C min^{-1} in N_2 with a flow rate of 60 cm^3 min^{-1}. The TMA experiments were conducted at least in duplicate to ensure the accuracy of the results. The TMA specimens were pellets of 10 mm diameter and ~1 mm thickness prepared by pressing powder of sample for 3 min under 8 kp cm^{-2} at ambient temperature. The T_g is assigned by the first inflection point in the TMA curve and it was obtained from the onset temperature of this transition during the second heating. Elemental analyses were carried out with a Carlo Erba model EA1108 analyzer.

2.2. Preparation of dyes

2.2.1. Dye TPAR3

A flask was charged with a mixture of **3** (0.36 g, 0.62 mmol), cyanoacetic acid (0.18 g, 2.11 mmol), dry acetonitrile (25 mL) and glacial acetic acid (1.5 mL). The mixture was stirred and refluxed for 15 h under N_2. It was subsequently concentrated and poured into water. The red precipitate was filtered, washed thoroughly with water and dried to afford TPAR3 (0.30 g, 63%).

FT-IR (KBr, cm^{-1}): 3430, 2970, 2214, 1718, 1592, 1484, 1444, 1318, 1288, 1224, 1182, 1058, 806.

^{1}H NMR ($CDCl_3$) ppm: 9.88 (s, 3H, COOH); 7.74 (m, 3H, elefinic); 7.35 (m, 6H, thiophene); 7.13 (m, 6H, phenylene meta to nitrogen); 7.04 (d, 6H, phenylene ortho to nitrogen).

Anal. Calcd. for $C_{42}H_{24}N_4O_6S_3$: C, 64.93; H, 3.11, N, 7.21. Found: C, 63.25; H, 3.04, N, 6.87.

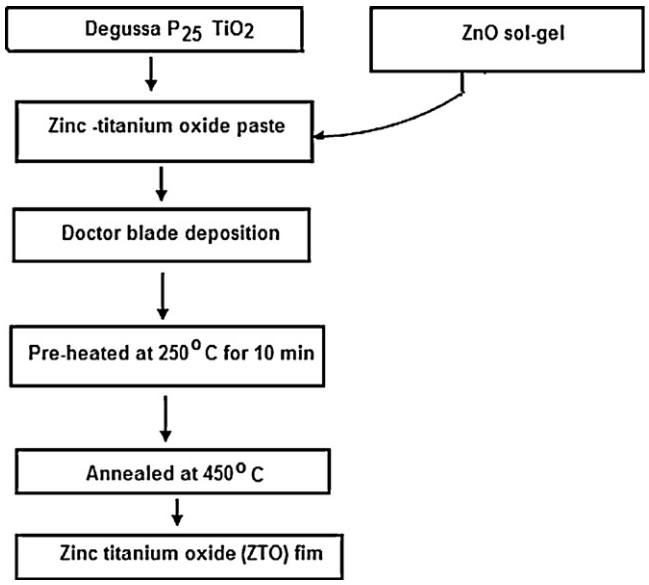

Fig. 1. Method for the preparation of zinc titanium oxide (ZTO) film.

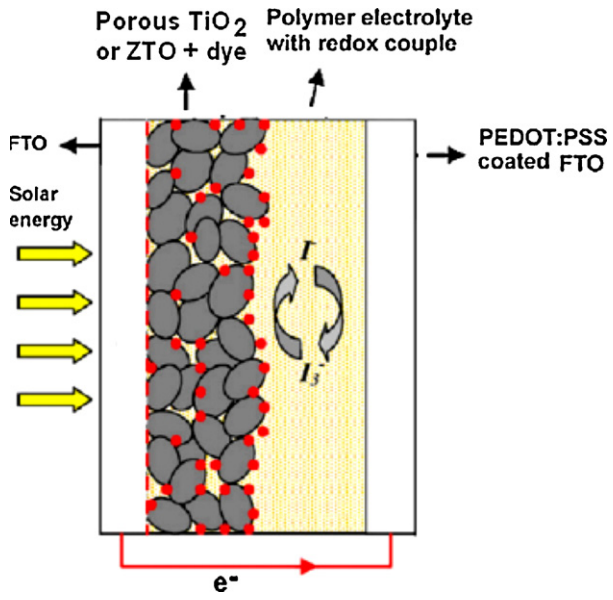

Fig. 2. Schematic diagram of quasi solid state DSSC with porous TiO_2 or ZTO + dye, polymer electrolyte with redox couple and PEDOT:PSS coated FTO counter electrode.

2.2.2. Dye BTDR2

BTDR2 was similarly prepared by reacting **7** (0.62 g, 1.74 mmol), with cyanoacetic acid (0.34 g, 4.00 mmol) in acetonitrile (30 mL) in the presence of a catalytic amount of glacial acetic acid (2 mL). BTDR2 precipitated from the reaction mixture as a red solid (0.65 g, 76%).

FT-IR (KBr, cm^{-1}): 3435, 2972, 2914, 2210, 1700, 1368, 1478, 1368, 1200, 810.

^1H NMR (DMSO-d_6) ppm: 10.07 (s, 2H, COOH); 7.83 (m, 2H, benzothiadiazole); 7.75 (s, 2H, olefinic); 7.21 (m, 4H, thiophene).

Anal. Calcd. for $C_{22}H_{10}N_4O_4S_3$: C, 53.87; H, 2.05, N, 11.42. Found: C, 53.06; H, 2.12, N, 11.38.

2.3. Preparation of sol–gel ZTO film and fabrication of quasi solid state dye-sensitized solar cells

ZnO sol–gel nanocrystalline power was prepared by dissolving zinc acetate dehydrate $(CH_3COO)_2Zn\ 2H_2O$ in methanol at room temperature. A clear solution of 0.5 M was obtained by magnetic stirring at 30 °C for 2 h. The pH value of solution was adjusted to 8 by adding desired amount of sodium hydroxide (0.1N) solution. The modified solution was again stirred for 1 h at room temperature. A clear solution was subsequently filtered through micron filter paper. The resulting transparent filtrate was kept for 3 h to complete the gelation and hydrolysis process. During this period, white ZnO precipitate was slowly crystallized and settled down at the bottom of the flask and then filtered and washed out with methanol to remove the starting material and then dried at 120 °C. The zinc titanium oxide (ZTO) nano-crystalline sol–gel was prepared by combining the titanium dioxide powder (P_{25}, a mixture of 30% rutile and 70% antase, Degussa, AG, Germany) with the above prepared ZnO sol–gel in methanol solution and then magnetically stirred and the paste was obtained. The films of ZTO were coated on FTO coated glass substrate by the doctor blade method. The crystalline structure of the ZTO nano-porous powder was measured using a PHILIPS X-ray diffractometer with CuKα radiation (λ_{Cu} = 1.54056 Å). The method of ZTO film preparation is shown in Fig. 1. We have also prepared nano-crystalline TiO_2 films using P_{25} paste in methanol by the doctor blade method. The thickness of the porous layer was controlled by adhesive tape. The porous thin films of TiO_2 or ZTO coated on FTO glass substrates were sintered at 450 °C for 30 min. After cooling the photoelectrodes to room temperature, the photoelectrodes were immersed in 5×10^{-4} M dye solution in THF and DMF to make the dye sensitized photoelectrodes with TPAR3 and BTDR2, respectively, for over night at room temperature.

The counter electrode was made by developing a thin film of PEDOT:PSS through spin coating, on the FTO glass substrate and then dried at 70 °C in air.

After the sensitization, a quasi solid state polymer electrolyte consisting of: LiI (0.1 g), I_2 (0.019 g), propylene carbonate (5 mL), P25 TiO_2 (0.0383 g), PEO (0.2648 g), and 4-*tert*-butylpyridine (0.044 mL) into acetonitrile (5 mL) solvent, was spread over the dye sensitized photoelectrode by spin coating to form the hole transporting layer. The DSSCs were made by clamping the photoelectrode consisting of polymer electrolyte with counter electrode. The schematic diagram of the DSSC is shown in Fig. 2. We have fabricated the following quasi solid state DSSCs: FTO/TiO_2-TPAR3/polymer electrolyte/PEDOT:PSS coated FTO (device A), FTO/ZTO-TPAR3/polymer electrolyte/PEDOT:PSS coated FTO (device B), FTO/TiO_2-BTDR2/polymer electrolyte/PEDOT:PSS coated FTO (device C) and FTO/ZTO-BTDR2/polymer electrolyte/PEDOT:PSS coated FTO (device D).

The current–voltage (*J–V*) characteristics in dark and under illumination were obtained by a Keithley electrometer (USA made) with built in power supply. A 100 W halogen lamp was used as light source and the intensity of the light is approximately of 100 mW cm^{-2} measured with the lux meter equipped with silicon detector. The electrochemical impedance spectra (EIS) measurements were carried out by applying bias of the open circuit voltage (V_{oc}) and recorded over a frequency range of 1 mHz to 10^5 Hz with ac amplitude of 10 mV. The above measurements were recorded with an Autolab Potentiostat PGSTAT-30 (Eco-Chemie, Netherlands) equipped with frequency response analyzer (FRA).

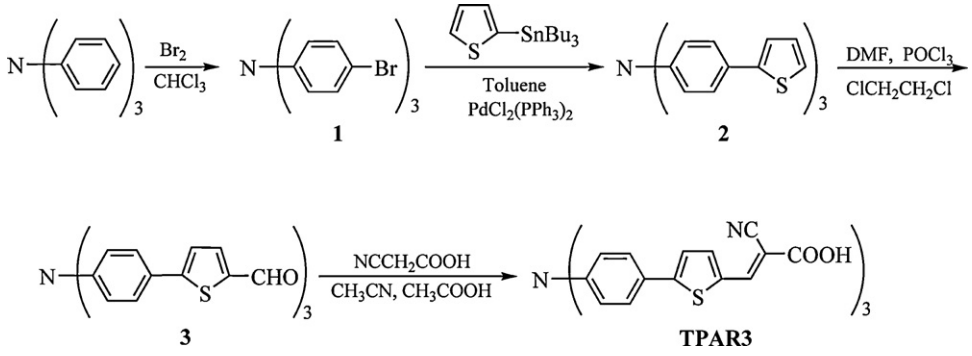

Scheme 1. Synthesis of TPAR3.

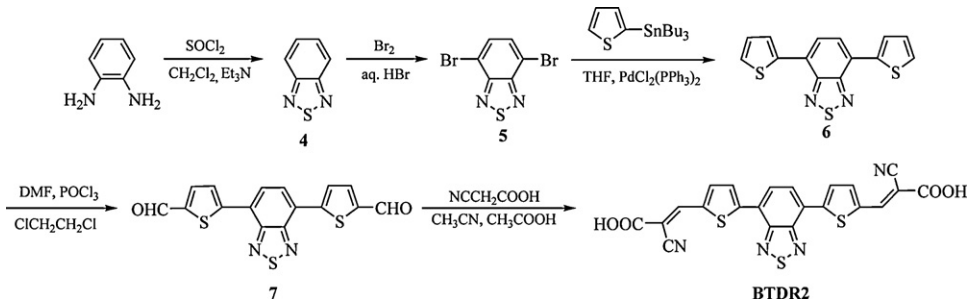

Scheme 2. Synthesis of BTDR2.

3. Results and discussion

3.1. Synthesis and characterization

The first dye, TPAR3, was prepared in moderate yields in four steps as illustrated in Scheme 1. The intermediate compounds **1** [37], **2** [38] and **3** [38,39] were synthesized according to the literature. Aldehyde **3** reacted with cyanoacetic acid in acetonitrile in the presence of a catalytic amount of glacial acetic acid to afford the required dye. TPAR3 is dark red in solid state and freely dissolves in common organic solvents even though it lacks of aliphatic chains. The three-dimensional structure of the triphenylamine core of this molecule is responsible for the enhanced solubility.

The second dye, BTDR2, was prepared by a five step synthetic route which is outlined in Scheme 2. Again, the intermediate compounds **4**, **5** [40], **6** [41] and **7** [38,39] were synthesized by known methods. Aldehyde **7** reacted with cyanoacetic acid, as was described above, to yield BTDR2 as a dark red solid. In contrast to TPAR3, the dye BTDR2 is almost insoluble in THF, chloroform and other common organic solvents. The central dithienyl-benzothiadiazole unit is almost coplanar, which also lacks of solubilizing aliphatic chains. BTDR2 dissolves only in strongly polar solvents with high boiling point, such as *N,N*-dimethylformamide (DMF) and dimethylsulfoxide (DMSO).

The binding mode of dye molecules to the TiO_2 surfaces, which is associated with interfacial electron injection was analyzed by FT-IR spectra. The FT-IR spectra of both dyes showed common characteristic absorption bands around at 3430, 2970 (O–H stretching of carboxyl); 1714 (C=O stretching of carbonyl); 2214 (cyano group); 1592, 1444 (aromatic) and 1058 cm^{-1} (out-of-plane deformation of trans olefinic bond). TPAR3 displayed an additional absorption at 1320 cm^{-1} assigned to the C–N stretching of triphenylamine. Finally, BTDR2 exhibited absorptions at 2914, 1478, 1368, 1200 and 810 cm^{-1} associated with the benzothiadiazole segment. It is observed that when both dyes were adsorbed onto the TiO_2 surface, the peak associated with O–H stretching of carboxyl group, disappeared. This observation shows that the deprotonation of COOH group is taking place on the TiO_2 surface, indicating the anchoring of the dye on the TiO_2 surface [17]. However, other main vibration bands are not influenced after the dye adsorption onto TiO_2 surface.

Fig. 3a presents the ^1H NMR spectrum of TPAR3 which showed an upfield signal at 9.88 ppm assigned to carboxyl. Furthermore, it showed resonances at 7.74 (olefinic "d"), 7.35 (thiophene "c"), 7.13 (phenylene "b") and 7.04 ppm (phenylene "a"). Finally, BTDR2 (Fig. 3b) displayed signals at 10.07 (carboxyl); 7.83 (benzothiadiazole); 7.75 (olefinic) and 7.21 (thiophene). It is noteworthy that the olefinic protons resonated at higher shift than the unsubstituted olefinic protons due to the deshielding effect of the electron-withdrawing cyano and carboxyl substituents.

Both dyes exhibited high thermal stability which was ascertained by TGA (Table 1). This property is attributable to the absence of solubilizing aliphatic chains in these molecules. The dyes had decomposition temperature (T_d) of 533–542 °C, char yields of 74–80% at 800 °C in N_2. Their glass transition temperature (T_g), which was determined by TMA, was 67–78 °C (Table 1). **BTDR2** was more thermally stable and rigid than TPAR3.

3.2. Photophysical properties

Fig. 4 presents the normalized UV–vis absorption spectra and the photoluminescence (PL) emission spectra in both dilute (10^{-5} M) THF solution and thin film. The latter was prepared by spin-coating on quartz substrate form THF solution for TPAR3 and from DMF solution for BTDR2. The UV–vis spectra were normalized with respect the long-wave absorption peak. All the photophysical characteristics of the dyes are summarized in Table 1.

Both dyes exhibited absorption bands at two distinct spectrum regions. Specifically, the absorption bands in the region below

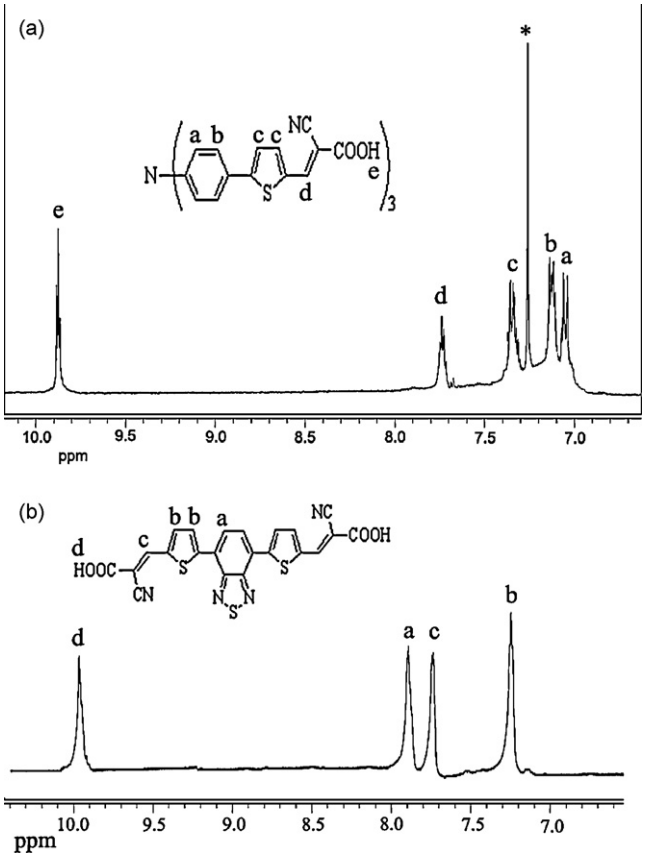

Fig. 3. (a) ^1H NMR spectrum of TPAR3 in $CDCl_3$ solution. The peak of the solvent is denoted with asterisk. (b) ^1H NMR spectrum of BTDR2 in DMSO-d_6 solution.

Table 1
Thermal, optical and electrochemical properties of dyes.

Dye	TPAR3	BTDR2
T_d[a] (°C)	533	542
Y_c[b] (%)	74	80
T_g[c] (°C)	67	78
$\lambda_{a,max}$[d] in solution (nm)	425	455
$\lambda_{a,max}$[d] in thin film (nm)	425	443
$\lambda_{f,max}$[e] in solution (nm)	547	565
$\lambda_{f,max}$[e] in solution (nm)	615	593
E_g^{opt}[f](eV)	2.10	2.17
HOMO (eV)	−5.38	−5.45
LUMO(eV)	−3.23	3.20
E_g^{el} [g](eV)	2.15	2.25

The emission spectra were obtained by excitation at 470 nm.
[a] Decomposition temperature corresponding to 5% weight loss in N_2 determined by TGA.
[b] Char yield at 800 °C in N_2 determined by TGA.
[c] Glass transition temperature determined by TMA.
[d] $\lambda_{a,max}$: the absorption maxima from the UV–vis spectra in THF solution or in thin film.
[e] $\lambda_{f,max}$: the emission maxima from the PL spectra in THF solution or in thin film.
[f] E_g^{opt} optical band gap determined from the absorption onset in thin film.
[g] E_g^{el} electrochemical band gap determined from cyclic voltammetry.

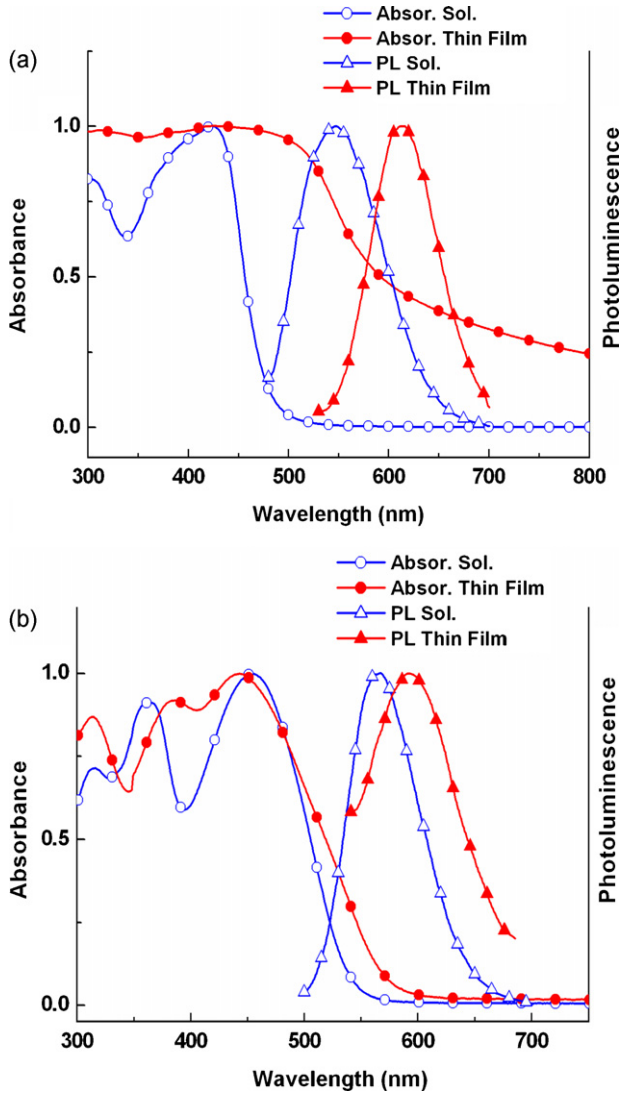

Fig. 4. Normalized UV–vis absorption and PL emission spectra in both THF solution and thin film of TPAR3 (a) and BTDR2 (b). The emission spectra were obtained by excitation at 470 nm.

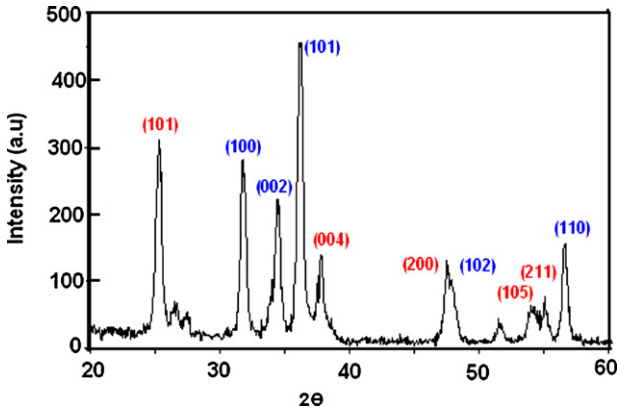

Fig. 5. XRD patterns of nano-crystalline zinc titanium oxide (ZTO) films annealed at 450 °C for 30 min in air. Red color planes' values indicate TiO_2 and blue color planes' values indicates ZnO. (For interpretation of the references to color in this figure legend, the reader is referred to the web version of the article.).

400 nm correspond to the π–π* electron transitions of the conjugated molecules. The absorption band above 400 nm is assigned to an intramolecular charge transfer (ICT) between the central unit and the cyanoacrylic acid anchoring moieties. More particularly, the dyes showed long-wave absorption maximum ($\lambda_{a,max}$) at 425 nm for TPAR3 and 443–455 nm for BTDR2. The $\lambda_{a,max}$ of BTDR2 was red shifted as compared to that of TPAR3. This indicates a greater electron delocalization in BTDR2 than TPAR3 even though triphenylamine is better electron donor than benzothiadiazole. The more coplanar structure of the benzothiadiazole favored the electron delocalization in BTDR2.

The optical band gaps (E_g^{opt}) of the dyes were determined from their absorption onset in thin film. In particular, the thin film absorption onset was located at 590 and 573 nm, which correspond to an E_g^{opt} of 2.10 and 2.17 eV for TPAR3 and BTDR2, respectively. Triphenylamine-based indoline dyes with multiple electron acceptors of rhodamine-3-acetic acid had shown band gaps of 2.17–2.34 eV [42].

By photoexcitation at 470 nm, the dyes emitted yellow-orange light with PL maximum ($\lambda_{f,max}$) at 547–615 nm (Fig. 4). A red shift was observed upon going from solution to thin film owing to the formation of aggregates.

The energy levels of the highest occupied molecular orbital (HOMO) and the lowest unoccupied molecular orbital (LUMO) of the dyes have also been estimated from the onset reduction potential and oxidation potentials, respectively observed in cyclic voltammogram (CV) data. These valves are summarized in Table 1. The value of energy band gap estimated from this data was also complied in Table 1 and is very close to the values estimated from the onset of optical absorption spectra.

3.3. Characterization of photoelectrodes

The X-ray diffraction (XRD) pattern of the ZTO film sintered at 450 °C for 30 min is shown in Fig. 5. The X-ray diffraction lines corresponded well to those for the tetragonal anatase phase of TiO_2 and wurtzite-type ZnO crystalline phase were observed and shown in the Fig. 5. The peaks at $2\theta = 25.25°$ (1 0 1), $2\theta = 37.82°$ (0 0 4), $2\theta = 47.98°$ (2 0 0), $2\theta = 53.59°$ (1 0 6), $2\theta = 55.07°$ (1 0 5) and $2\theta = 55.12°$ (2 1 1), are all attributable to the anatase phase of TiO_2 compare with JCPDS Card No: 21-1272. Then additionally, other peaks belonging to (1 0 0), (0 0 2), (1 0 1), and (1 1 0) planes confirm the formation of a wurtzite-type ZnO compare with JCPDS standard data 36-1451.

The absorption spectra of TPAR3 and BTDR2 dye adsorbed on TiO_2 film are shown in Fig. 6a and b, respectively. When dyes

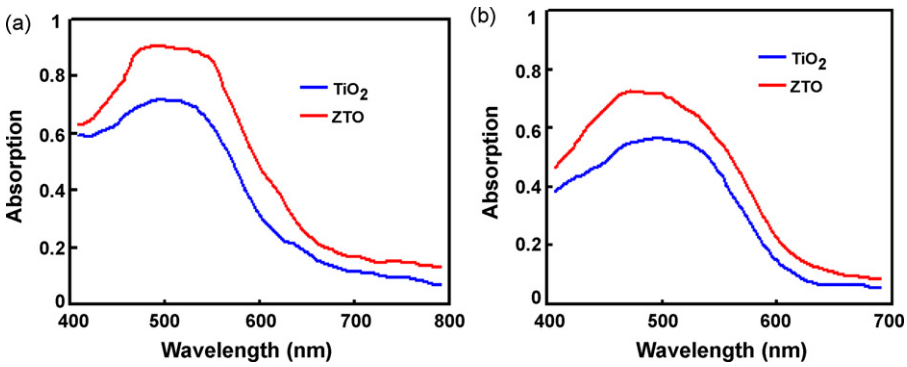

Fig. 6. Absorption spectra of (a) TPAR3 (b) BTDR2 dye sensitized TiO_2 and ZTO electrodes.

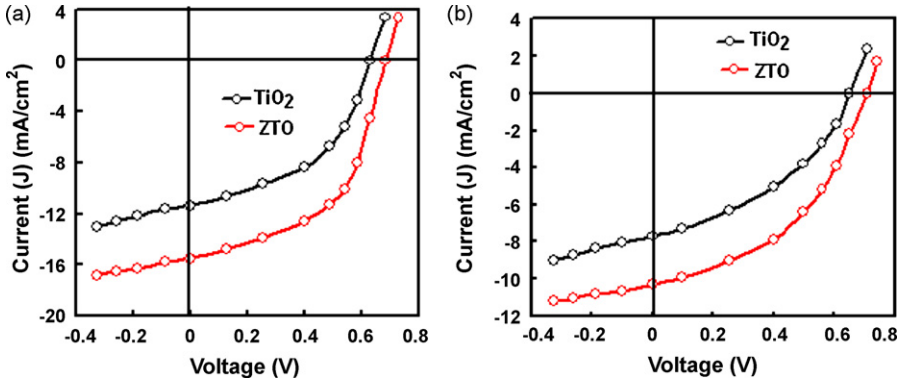

Fig. 7. Current–voltage characteristics of the quasi-solid state DSSCs based on (a) TRAR3 and (b) BTDR2 dyes, using TiO_2 and ZTO photoelectrodes.

adsorbed on the TiO_2 surface, the absorption spectra were broadened and red shifted in relative to the absorption spectra of the dye, indicating that most of the dye molecules absorbed on the TiO_2 surface with only partially *J*-aggregation on nano-crystalline surface. The broadening of the absorption spectra is due to an interaction between the dye and TiO_2 [14]. The absorption spectra of TPAR3 dye adsorbed on ZTO electrode are also shown in Fig. 6. As can be seen from Fig. 6a and b, the dye absorption by ZTO electrode has been increased as compared to the TiO_2 electrode, indicating an increase in the surface area of ZTO film for dye adsorption. The maximum peak for dye absorption in ZTO electrode also slightly blue shifted as compared to TiO_2 electrode. This blue shift results from the increased surface basicity due to ZnO nanoparticles. This means the surface of ZTO electrode is more basic than that of TiO_2 leading to significant improvement in the dye absorption.

3.4. Photovoltaic properties of the quasi solid state dye sensitized solar cells

Fig. 7 shows the current density–voltage (*J*–*V*) curves under illumination of 10 mW cm^{-2} for quasi solid state DSSCs prepared using TiO_2 and ZnO–TiO_2 (ZTO) composite film photoelectrodes using TPAR3 and BTDR2 dyes. The photovoltaic parameters estimated from these curves are complied in Table 2. It is observed that both the short circuit photocurrent (J_{sc}) and the open circuit voltage (V_{oc}) for DSSC based on TPAR3 dye are higher than those for BTDR2 under same conditions. This improvement in V_{oc} may be related to the increase in electron life time in the DSSC by preventing the dark current. The higher LUMO level of TPAR3 is also beneficial for the higher value of V_{oc} [43]. The increase in J_{sc} may be the reduction in reorganizing energy of the TPAR3 [44] and also the higher amount of TPAR3 dye adsorbed on the nanocrystalline electrodes as compared to BTDR2 observed in Fig. 6. It can be seen from Table 1 that both J_{sc} and V_{oc} for the devices fabricated on ZTO photoelectrodes are higher than those for bare TiO_2 electrodes. The increase in J_{sc} is consistent with the absorption spectra of the dyes sensitized ZTO electrode as shown in Fig. 6. This increased surface area provides additional absorption sites for the dye, which contributes to the light harvesting efficiency of the photoelectrode that results an improvement in J_{sc}. The incident photon to current efficiency (IPCE) spectra of the DSSCs are shown in Fig. 8a and b, using TPAR3 and BTDR2 dyes, respectively. The value of IPCE for the DSSC with TPAR3 is higher than that for BTDR2 in the wavelength range of 430–560 nm. This may be due to the increased absorption of the TPAR3 in this region.

From Table 1, it is evident that both J_{sc} and V_{oc} are higher for the DSSCs with ZTO photoelectrode than that for bare TiO_2 photoelectrode. As a result of these changes, the overall power conversion efficiency (η) of the cell containing ZTO photoelectrode increased

Table 2
Detail photovoltaic performance of different quasi solid state dye sensitized solar cells.

Device	Short circuit current (J_{sc}) (mA/cm^2)	Open circuit voltage (V_{oc}) (V)	Fill factor (FF)	Power conversion efficiency (η) (%)
A	10.2	0.70	0.55	3.9
B	15.6	0.76	0.59	6.3
C	7.72	0.65	0.45	2.42
D	10.34	0.71	0.51	3.6

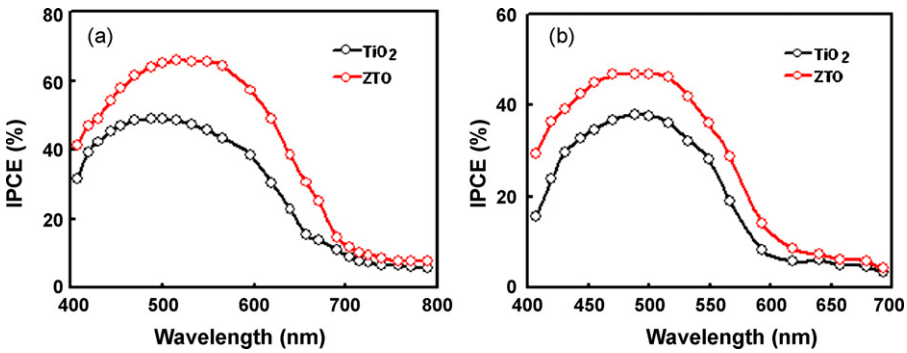

Fig. 8. IPCE spectra of the quasi-solid state DSSCs based on (a) TRAR3 and (b) BTDR2 dyes, using TiO_2 and ZTO photoelectrodes.

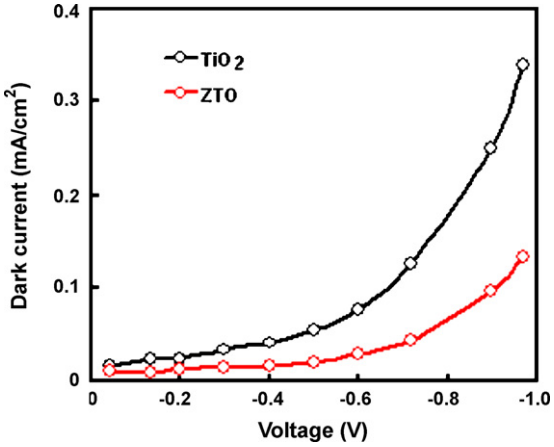

Fig. 9. Current–voltage (revere bias) characteristics of quasi-solid state DSSCs employing TPAR3 dye with different nanocrystalline photoelectrodes.

to 3.6% from 2.42% and to 6.3% from 3.9% based on BTDR2 and TPAR3 dyes, respectively, with respect to the bare TiO_2 electrode. The increase shown by the ZTO cell was found to be consistent with the increased amount of the dye adsorbed on the ZTO film as shown in Fig. 6.

The increased J_{sc} may be due the enhanced light scattering by ZTO film through extending the distance traveled by light that results an increase in light harvesting efficiency by the electrode relative to that by the TiO_2 film. Fig. 9 shows that the corresponding dark current for DSSC containing ZTO photoelectrode with TPAR3 dye, is low relative to that for bare TiO_2 photoelectrode. The observed decrease in dark current is essential due to the suppression of I_3^- reduction at the dye sensitized TiO_2 electrodes. This also favors reduction of back electron transfer and consequently increases the V_{oc}. The increase in the energy barrier at the ZTO/electrolyte interface reduces the dark current due to the reduction in the back electron transfer from the conduction band of ZTO to I_3^- in the electrolyte. Although the dark current in DSSCs cannot be considered as a direct measurement of the recombination process, it can be used to measure the conduction band edge shift. As shown in Fig. 9, the onset potential shifts towards the more negative voltage (−0.4 V for TiO_2 and −0.6 V for ZTO), indicating that the conduction band edge in ZTO shifts upward direction towards the vacuum level.

The value of the incident photon to current efficiency (IPCE) for the DSSC with ZTO photoelectrode is higher than that for the bare TiO_2. The IPCE can also be expressed by the following expression [45]:

$$\mathrm{IPCE}(\lambda) = \mathrm{LHE}(\lambda)\varphi_{\mathrm{inj}}\eta_{\mathrm{c}} \quad (1)$$

where LHE (λ) is the light harvesting efficiency, φ_{inj} is the quantum yield of the electron injection from the excited dyes to the conduction band of metal oxide semiconducting film used in the photoelectrode and η_c is the efficiency of the photo-injected electrons at the back contact. The factor LHE (λ), related to the dye uptake by the photoelectrode surface is significant in the present devices. Since the amount of the dye adsorbed by the ZTO photoelectrode is more than that for TiO_2 photoelectrode, the LHE is responsible for the enhancement in the IPCE of the DSSC. Because the φ_{inj} is related to the energetic discrepancy between the conduction band of metal oxide semiconductor used in photoelectrode and the excited level of dye, the large difference creates a driving force, which facilitates charge transfer from the excited dye molecules to the conduction band of metal oxide semiconductor [46]. The negative shift in the V_{cb} in ZTO photoelectrode has been confirmed by the observed blue shift in the wavelength showing maximum absorption intensity.

The electrochemical impedance spectroscopy (EIS) has been widely used to study the kinetics of electrochemical processes occurring in the DSSCs [47]. Fig. 10a shows Nyquist plots of EIS of DSSCs using TiO_2 and ZTO electrodes employing TPAR3 dyes as sensitizer, in complex plane. Z_1 and Z_2 are impedances related to charge transfer processes at the surface of counter electrode and at

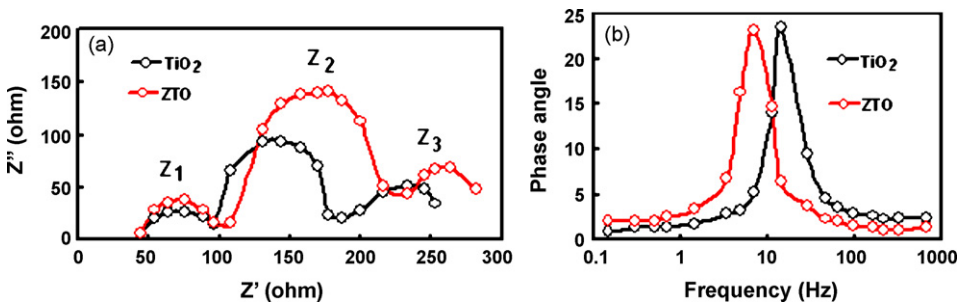

Fig. 10. (a) Nyquist plots and (b) Bode plots of quasi solid state DSSCs employing TPAR3 dyes with TiO_2 and ZTO photoelectrodes.

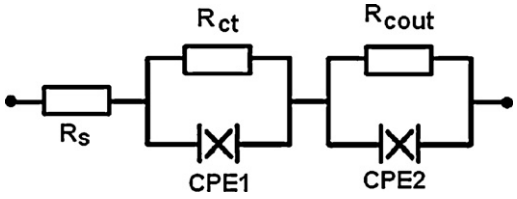

Fig. 11. Equivalent circuit of the device.

the TiO_2 or ZTO/dye/electrolyte interface, respectively. Z_3 is related to the redox diffusion within the electrolyte [48–50]. The larger semicircle corresponds to the Z_2 is attributed to the charge transfer at nanocrystalline electrode/electrolyte interface and the ion diffusion of redox species in the electrolyte. Fitting this semicircle with the equivalent circuit shown in Fig. 11, subsequently gives the charge transfer resistance (R_{ct}) and the chemical capacitance (C_μ) at the nanocrystalline electrode/electrolyte interface. The value of R_{ct} for the DSSC based on TiO_2 electrode (85 Ω) is lower than that for ZTO electrode (115 Ω), indicating the higher charge losses in the TiO_2/electrolyte interface. As the large charge losses limit the V_{oc} to lower values, the DSSCs with TiO_2 electrode shows lower value of V_{oc} as compared to DSSC with ZTO.

The estimated values of chemical capacitance for the EIS spectra, at the interface TiO_2/electrolyte and ZTO/electrolyte are about 156 and 185 μF, respectively. The chemical capacitance of the nanostructured electrode DSSC has been expressed as [51]:

$$C_\mu = \frac{q^2}{kT} \exp\left[\frac{\alpha q}{kT}(E_F - E_{cb})\right] \quad (2)$$

where E_F is the position of the Fermi level of the electrons, E_{cb} is the position of conduction band, q is the electronic charge, k is the Boltzmann's constant, T is the absolute temperature and α is a constant related to the distribution of electronic states below the conduction band. The higher value of chemical capacitance indicates a higher density of accessible electronic states at the surface. As it can be seen from the above equation, the increase in the capacitance is also caused by the negative shift in the conduction band position of nanostructured electrode, which agrees with the lager short circuit current observed in the DSSC based on ZTO nanostructured electrode.

We have estimated the values of electron life time (τ_n) from the product of R_{ct} and C_μ and the values are 13 and 21 ms for DSSC employing TiO_2 and ZTO electrodes. The Bode plots of EIS Spectra (mid frequency range) are shown in Fig. 10b. The frequency peak related to the ZTO electrode shifted towards the lower frequency side relative to TiO_2 electrode. The electron lifetime has been estimated from the expression $\tau_n = 1/2\pi f_{max}$, where f_{max} is the peak frequency and found to be 12 and 23 ms for DSSCs with ZTO and TiO_2 respectively. These values are in good agreement estimated from the Nyquist plots of EIS spectra. The increase in τ_n is associated with a rise in both R_{ct} and C_μ, which indicates that using ZTO photoelectrode, decrease the interfacial recombination rate for electrons with triiodide ions. This may the one of the reason for the improvement in the power conversion efficiency of the DSSCs with ZTO photoelectrode.

4. Conclusions

We demonstrated triphenylamine- or benzothiadiazole-based metal-free dyes that can be used as light sensitizers for DSSCs. **TPAR3** was soluble in common organic solvents, while **BTDR2** dissolved only in DMF. Both dyes displayed high thermal stability and moderate glass transition temperature. The absorption maximum of **BTDR2** was red shifted relative to **TPAR3**. The optical band gap of the dyes was ~2.10 eV.

We have investigated the photovoltaic performance of the quasi solid state DSSCs with these dyes as photosenisiters, TiO_2 or ZTO as photoelectrodes and PEDOT:PSS coated FTO as counter electrode. It was found that the DSSCs with TPAR3 shows higher power conversion efficiency as compared to BTDR2 which was attributed to the higher light harvesting efficiency of TPAR3. The overall power conversion efficiency of the quasi solid state DSSCs using TPAR3 dye with ZTO electrode is about 6.3% as compared to 3.6% with TiO_2 photoelectrode. The improvement is attributed to the enhancement in the electron lifetime and reduction in recombination rate. This investigation also draws attention that employing ZTO (composite of ZnO and TiO_2 nanocrystallines) enhances the photovoltaic performance by not only shifting the conduction band edge to negative potential as compared to TiO_2 but also shield its surface recombination.

References

[1] B. O'Regan, M. Grätzel, Nature 353 (1991) 737.
[2] M.K. Nazeeruddin, A. Kay, I. Rodicio, R. Humphry-Baker, E. Muller, P. Liska, N. Vlachopoulos, M. Grätzel, J. Am. Chem. Soc. 115 (1993) 6382.
[3] S.Y. Huang, G. Schlichthorl, A.J. Nozik, M. Grätzel, A.J. Frank, J. Phys. Chem. B 101 (1997) 2576.
[4] T. Oekermann, D. Zhang, T. Yoshida, H. Minoura, J. Phys. Chem. B 108 (2004) 2227.
[5] G. Boschloo, A. Hagfeldt, J. Phys. Chem. B 109 (2005) 12093.
[6] M. Grätzel, Inorg. Chem. 44 (2005) 6841.
[7] Z.S. Wang, K. Hara, Y. Dan-oh, C. Kasada, A. Shinpo, S. Suga, H. Arakawa, H. Sugihara, J. Phys. Chem. B 109 (2005) 3907.
[8] http://kuroppe.tagen.tohoku.ac.jp/(dsc/cell-e.htm.
[9] T. Kitamura, M. Ikeda, K. Shigaki, T. Inoue, N.A. Anderson, X. Ai, T.Q. Lian, S. Yanagida, Chem. Mater. 16 (2004) 1806.
[10] D.P. Hagberg, T. Edvinsson, T. Marinado, G. Boschloo, A. Hagfeldt, L.C. Sun, Chem. Commun. (2006) 2245.
[11] V. Shklover, Y.E. Ovchinnikov, L.S. Braginsky, S.M. Zakeeruddin, M. Grätzel, Chem. Mater. 10 (1998) 2533.
[12] S. Ito, S.M. Zakeeruddin, R. Humphry-Baker, P. Liska, R. Charvet, P. Comte, M.K. Nazeeruddin, P. Peéchy, M. Takata, H. Miura, S. Uchida, M. Grätzel, Adv. Mater. 18 (2006) 1202.
[13] K. Hara, T. Sato, R. Katoh, A. Furube, Y. Ohga, A. Shinpo, S. Suga, K. Sayama, H. Sugihara, H. Arakawa, J. Phys. Chem. B 107 (2003) 597.
[14] K. Hara, M. Kurashige, Y. Dan-oh, C. Kasada, A. Shinpo, S. Suga, K. Sayama, H. Arakawa, New J. Chem. 27 (2003) 783.
[15] M. Liang, W. Xu, F.S. Cai, P. Chen, B. Peng, J. Chen, Z.M. Li, J. Phys. Chem. C 111 (2007) 4465.
[16] W. Xu, B. Peng, J. Chen, M. Liang, F.S. Cai, J. Phys. Chem. C 112 (2008) 874.
[17] J. Pei, S. Peng, J. Shi, Y. Liang, Z. Tao, J. Liang, J. Chen. J. Power Sources 187 (2009) 620.
[18] H. Tian, X.C. Yang, R.K. Chen, R. Zhang, A. Hagfeldt, L.C. Sun, J. Phys. Chem. C 112 (2008) 11023.
[19] F. Zhang, Y. Luo, J. Song, X. Guo, W. Liu, C. Ma, Y. Huang, M. Ge, Z. Bo, Q. Meng, Dyes Pigments 81 (2009) 224.
[20] Z.J. Ning, Q. Zhang, W.J. Wu, H.C. Pei, B. Liu, H. Tian, J. Org. Chem. 73 (2008) 3791.
[21] M. Velusamy, K.R. Justin Thomas, J.T. Lin, Y.C. Hsu, K.C. Ho, Org. Lett. 7 (2005) 1899.
[22] X. Ma, J. Hua, W. Wu, Y. Jin, F. Meng, W. Zhan, H. Tian, Tetrahedron 64 (2008) 345.
[23] D.P. Hagberg, J.-H. Yum, H. Lee, F. De Angelis, T. Marinado, K.M. Karlsson, R. Humphry-Baker, L. Sun, A. Hagfeldt, M. Grätzel, et al., J. Am. Chem. Soc. 130 (2008) 6259.
[24] P. She, Y. Liu, X. Huang, B. Zhao, N. Xiang, J. Fei, L. Liu, X. Wang, H. Huang, S. Tan, Dyes Pigments 83 (2009) 187.
[25] C. Yang, H. Chen, C. Chen, S. Liao, H. Hsiao, Y. Chuang, H. Hsu, T. Wang, Y. Shieh, L. Lin, Y. Tsai, J. Electroanal. Chem. 631 (2009) 43.
[26] M. Velusamy, K.R.J. Thomas, J.T. Lin, Y. Hsu, K. Ho, Org. Lett. 7 (2005) 1899.
[27] W. Shin, S. Kim, S. Lee, H. Jeon, M. Kim, B. Naidu, S. Jin, J. Lee, J. Lee, Y. Gal, J. Polym. Sci. Part A: Polym. Chem. 45 (2007) 1394.
[28] J. Oshita, S. Kangai, H. Yoshida, A. Kunai, S. Kajiwara, Y. Ooyama, Y. Harima, J. Organometall. Chem. 692 (2007) 801.
[29] J. Kim, H. Choi, J. Lee, M. Kang, K. Song, S. Kang, J. Ko, J. Mater. Chem. 18 (2008) 5223.
[30] Z.S. Wang, C.H. Huang, Y.Y. Huang, Y.J. Hou, P.H. Xie, B.W. Zhang, H.M. Cheng, Chem. Mater. 13 (2001) 678.
[31] I. Saeki, J. Setaka, R. Furuitchi, H. Konno, J. Electroanal. Chem. 464 (1999) 238.
[32] X. Wu, L. Wang, F. Luo, B. Ma, C. Zhan, Y. Qiu, J. Phys. Chem. C 111 (2007) 8075.
[33] H.X. Wang, H. Li, B.F. Xue, Z.X. Wang, Q.B. Meng, L.Q. Chen, J. Am. Chem. Soc. 127 (2005) 6394.
[34] M.S. Kang, J.H. Kim, J. Won, Y.S. Kang, J. Photochem. Photobiol. A 183 (2006) 15.
[35] Y.J. Kim, J.H. Kim, M.S. Kang, M.S. Lee, J. Won, J.C. Lee, Y.S. Keng, Adv. Mater. 16 (2004) 1753.

[36] J.N. deFreitas, A. de Souza Goncalves, M.A. De paoli, J.R. Durrant, A.F. Nogueira, Electrochim. Acta 53 (2008) 7166.
[37] J. Cremer, P. Baeuerle, J. Mater. Chem. 16 (2006) 874.
[38] S. Roquet, A. Cravino, P. Leriche, O. Alévêque, P. Frère, J. Roncali, J. Am. Chem. Soc. 128 (2006) 3459.
[39] J.A. Mikroyannidis, M.M. Stylianakis, P. Suresh, P. Balraju, G.D. Sharma, Org. Electron. 10 (2009) 1171.
[40] F.S. Mancilha, B.A. DaSilveira Neto, A.S. Lopes, P.F. Moreira Jr., F.H. Quina, R.S. Gonçalves, J. Dupont, Eur. J. Org. Chem. 21 (2006) 4924.
[41] C. Kitamura, S. Tanaka, Y. Yamashita, Chem. Mater. 8 (1996) 570.
[42] C.-H. Yang, H.-L. Chen, Y.-Y Chuang, C.-G. Wu, C.-P. Chen, S.-H. Liao, T.-L. Wang, J. Power Sources. doi: 10.1016.
[43] W. Xu, J. Pei, J. Shi, S. Peng, J. Chen, J. Power Sources 183 (2008) 792.
[44] N. Koumura, Z.S. Wang, S. Mori, M. Miyashita, E. Suzuki, K. Hara, J. Am. Chem. Soc. 128 (2006) 14256.
[45] J. Halme, G. Boschloo, A. Hagfeldt, P. Lund, J. Phys. Chem. C 112 (2008) 5623.
[46] A.J. Frank, N. Kopidakis, J. van de Lagemaat, Coord. Chem. Rev. 248 (2004) 1165.
[47] F. Fabregat-Santiago, J. Bisquert, G. Garcia-Belmonte, G. Boschloo, A. Hagfeldt, Sol. Energy Mater. Sol. Cells 87 (2005) 117.
[48] R. Kern, R. Sastrawan, J. Ferber, J. Luther, Electrochem. Acta 47 (2002) 4213.
[49] Q. Wang, J.E. Moser, M. Grätzel, J. Phys. Chem. B 109 (2005).
[50] L. Han, N. Koide, Y. Chiba, A. Islam, R. Komiya, N. Fuke, A. Fukui, R. Yamanaka, Appl. Phys. Lett. 86 (2005) 213501.
[51] J. Bisquert, Phys. Chem. Chem. Phys. 5 (2003) 5360.